Sakarya University Journal of Science
SAUJS

Title: Determination of the Dynamic Properties of SDOF and MDOF Shear Frames with Image Processing Technique

Authors: Erdem DAMCI, Çağla ŞEKERCİ

Determination of the Dynamic Properties of SDOF and MDOF Shear Frames with Image Processing Technique

Erdem DAMCI [*1] , Çağla ŞEKERCİ[1,2]

Abstract

In this study, experimental modal analyses on shear frame models consisting of single and multi-degree-of-freedom structure models were carried out to examine structural behavior. The image processing technique is used for the tests on shaking tables, such as free vibration, simple harmonic, and strong ground motion. An approach is proposed for image processing techniques to consider the appropriate filter size. The experiments aimed to determine the displacements at the floor levels and the dynamic characteristics of the structure models. To determine the displacements and frequency responses, results obtained from three different methods, namely the data obtained by accelerometers, image processing technique, and theoretical calculations, were compared. It has been shown that the image processing technique is a good tool compared to frequently used vibration measurements with accelerometers. It is advantageous because it is easier to implement for laboratory experiments and less costly.

Keywords: Image processing, dynamic characteristics, shear frames

1. INTRODUCTION

The image processing technique has become popular in determining parameters such as displacement and stress distribution in many engineering fields. It has become very popular in the field of civil engineering. It is also a cost-effective and easy-to-use method compared to other experimentally preferred methods. Stress distribution of fractures and cracks can be examined in material sciences. In a study on material mechanics, the thermal deformation of steel beams at different temperatures and times was determined by an image processing technique [1]. Also, structural engineering has been used to determine the dynamic characteristics of structures (period, mode shapes, damping ratio) and the displacements and rotations at a selected point. In a study, the static and dynamic displacements of the Humber Bridge in England were determined based on the analysis of the images taken with a camera capable of shooting up to 1000 fps considering the roundel targets placed on the bridge [2]. In recent studies, displacements at selected points on the bridges were determined with an image processing technique, and it was mentioned that it gives more accurate results and easier application than the other methods [3–5].

* Corresponding author: edamci@iuc.edu.tr (E. DAMCI)
[1] Faculty of Engineering, Department of Civil Engineering, İstanbul University-Cerrahpaşa, İstanbul, Türkiye
[2] Faculty of Engineering, Department of Civil Engineering, Doğuş University, İstanbul, Türkiye
E-mail: csekerci@dogus.edu.tr
ORCID: https://orcid.org/0000-0003-2295-1686, https://orcid.org/0000-0001-7070-1804

Erdem DAMCI, Çağla ŞEKERCİ

Determination of the Dynamic Properties of SDOF and MDOF Shear Frames with Image Processing Technique...

In a study to determine the deviations that may occur in the horizontal direction of high-rise buildings, the displacements were obtained from the focal shifts of the cameras placed parallel to a flexible steel column and the changes in the camera angles in the laboratory environment [6]. In the studies performed with the image processing technique, shaking table tests or pulse-induced vibrations were conducted and analysed, and the resulting displacements were determined [7–9].

In addition, in studies where motion detection systems are established, and the movements of selected points are determined and measurements using high-resolution cameras to determine displacements, it is emphasised that it is possible to perform better and lower cost measurements than the vibration sensors [10–15]. In the determination of displacements, measurements have been made using not only image processing but also laser displacement sensors, and in an examined comparative study, it has been reported that the margin of error was minimum [16]. Different image processing techniques are used for operational modal analyses and damage detection on small-scale structure models in laboratory environments [17]. There are also studies in which image processing is used for structural health monitoring [18–20].

2. MATERIALS AND METHOD

2.1. Properties of Shear Frames

The total height of the designed shear frames is 75 cm, including a single-degree-of-freedom (SDOF) model and a two-story multi-degree-of-freedom (MDOF) model. In order to reduce the column end rotations to the degree that can be neglected at the floor levels and to ensure that the system behaves like an actual shear frame, to obtain a relatively rigid floor, medium-density fiberboard (MDF) plates 36 mm thick and dimensions of 100 x 150 mm were used. In order to minimise out-of-plane displacements and to force the frame deflections in one direction under desired vibrations, columns are designed with aluminium sheets in a thickness of 2 mm, where the width is 100 mm, and the height is 750 mm. Three holes opened on the columns with 3 mm diameter for wood screws were considered while calculating the shear stiffness.

2.2. Experimental Setup and Test Equipment

Both SDOF and MDOF shear frames were subjected to 3 different tests. The first of the experiments is the free vibration test, one of the easiest-to-implement methods for determining dynamic characteristics. Video and acceleration recordings were taken during free vibration tests by giving an initial displacement to the top floors of the structures. The models' dynamic characteristics were determined by video processing and vibration analysis and compared with theoretical results.

Besides, using the model update technique, the actual flexural rigidity of the columns is also determined. Instead, two other experiments were conducted to establish forced vibration tests using a shake table [21] for earthquake and harmonic motion simulations. These experiments aim to compare the theoretical results with the displacement-time histories of the models obtained by video processing under harmonic and earthquake simulations.

For the experimental study, the setup given in Figure 1 was established. In order to obtain the vibration recordings, two accelerometer devices built with an Arduino Nano board and an MPU6050 sensor are mounted to each floor level (Figure 2). These accelerometers are calibrated using Earth's gravity prior to each experiment. The sensitivity of the sensors is set to 2g and 4g ranges according to the desired response of the structure model. The sampling rate of the assembled system is about 200 Hz, which is enough for obtaining a smooth and dynamically sufficient

Erdem DAMCI, Çağla ŞEKERCİ

Determination of the Dynamic Properties of SDOF and MDOF Shear Frames with Image Processing Technique...

acceleration-time history. Each record was filtered using the SeismoSignal [22] software, and the dominant frequencies were determined by power spectrum. It must be filtered for adequate accuracy in obtaining a displacement-time history from acceleration recordings. Several experiments conducted with the MPU6050 sensor have shown that using a Butterworth fourth-order band-pass filter with 1 Hz low-cut and 20 Hz high-cut values gives good results.
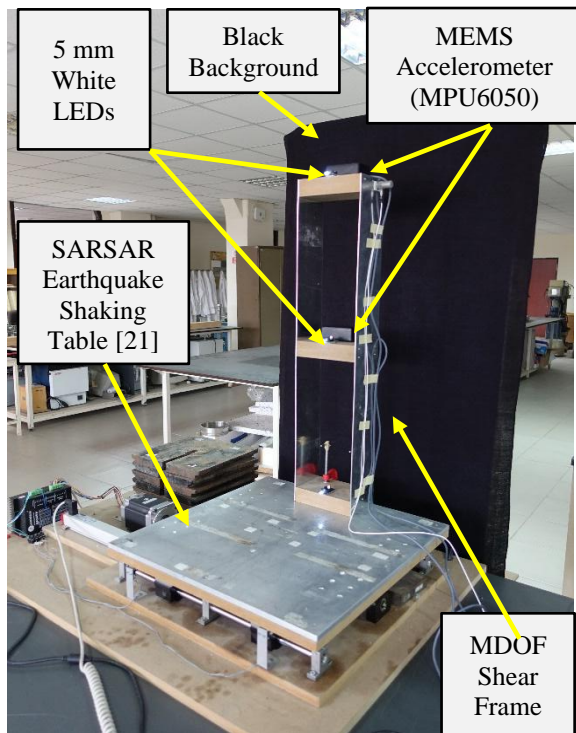
Figure 1 General view of the experimental setup

Figure 2 Outside (left) and inside (right) views of the low-cost Arduino-based accelerometers

For image processing, three 5 mm white LED indicators with light intensity higher than the environment are positioned to determine the displacements at ground and floor levels. A black background was used to facilitate filtering the LEDs according to the determined intensity threshold value. Sony RX100-M5 model 4K and high fps camera is used for video recordings.

2.3. Video Processing Technique

In the video processing process, videos recorded at 100 fps rate were converted to pixel-time and displacement-time histories with a program written in MATLAB [23]. Each video recorded for image processing was divided into 100 frames per second, and the individual LEDs' positions were considered separately. White LEDs were placed at the control points where displacements were desired to calculate. In order to track white LEDs more efficiently, first, video frames with RGB images were converted into grey-scale by using the B component of RGB images and then binarised by the Otsu

Thresholding Method with a specified intensity threshold value (i=0.99). In the binarisation process, the pixels below the threshold value were converted to black, and the ones above this value were converted to white pixels. Also, if it exists to neglect unrelated white pixels, the BW area open filter was applied by a post process. Following these processes, a median filter is applied to smoothen the geometry of the white LED pixel areas. As a result of this process, only the LED lights were left in each frame for tracking to obtain pixel-time data (Figure 3). At this point, determining the accurate median filter size is essential for precise displacement tracking. For this purpose, to determine the appropriate median filter size in each frame for each LED, the diameter (D) of the LEDs is observed and calculated first. Choosing an odd limit value of ¾D for each LED's filter size, each frame was analysed for all odd numbers starting from 3 to ¾D, and the centroid of the filtered LEDs was calculated to condense white pixels into one point for gathering the pixel-time history of each floor in x-y coordinate system.

Erdem DAMCI, Çağla ŞEKERCİ

Determination of the Dynamic Properties of SDOF and MDOF Shear Frames with Image Processing Technique...

Sample video frames considering these stages for four different filter sizes are given in Figure 4, and plotted centroids for all median filter sizes are given in Figure 5. The nearest point to the average of all coordinates is calculated in each frame to estimate an appropriate median filter size. Considering these calculations for optimum median filter size, the most frequent value of median filter size was used for displacement tracking in all frames (Figure 6).
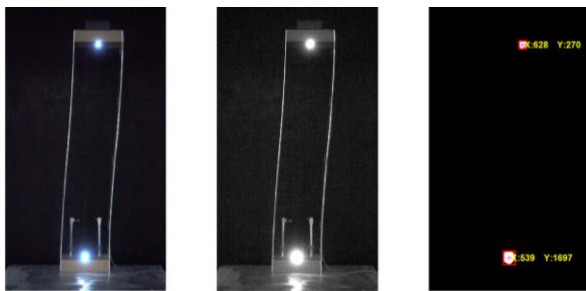
Figure 3 Image processing steps: Original image (left), Blue component (middle), filtered image for the specified intensity threshold value (right).
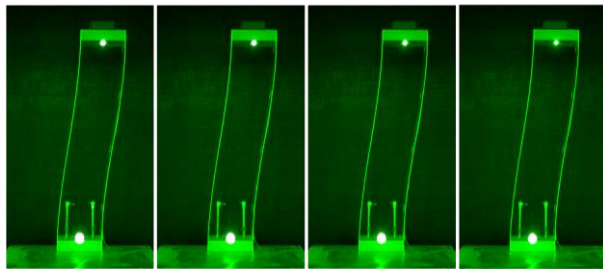
Figure 4 Processing of a sample video frame for median filter sizes 21, 31, 41, and 51 from left to right, respectively.

After this optimisation process, using the determined median filter size, pixel-to-displacement data was also obtained by measuring a known length of a structural member from a video frame in pixels to scale displacements in mm/pixel units. Finally, pixel-time and displacement-time histories were obtained by combining all frames in 1/100 sec divisions.
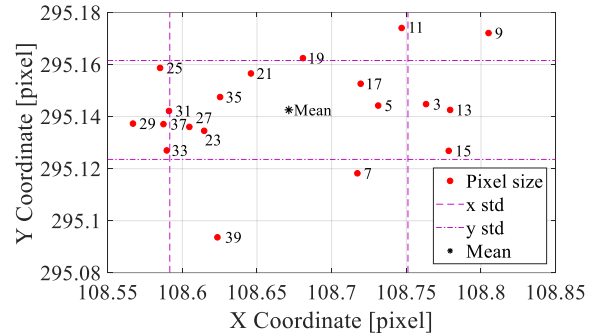
Figure 5 Calculated centroids of a sample frame for median filter from 3 to ¾D pixel sizes at bottom floor LED
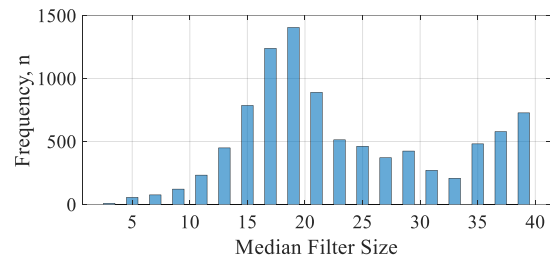
Figure 6 Number of median sizes nearest to mean in each frame for determining the optimum size

2.4. Numerical Analysis Methods

The dynamic characteristics of the shear frames are determined using a numerical analysis with the lumped mass assumption, considering the additional masses of the accelerometers and the mounted LEDs. The mass in the SDOF system is determined by calculating half of the mass of the bare shear frame, which is assumed to be concentrated at the top floor with the addition of an accelerometer and LED masses. For the MDOF system, half of the mass of the bare shear frame is concentrated at the mid-floor, and ¼ of the total mass was considered at the top floor with additional masses of accelerometers and LEDs.

Another parameter affecting the natural frequency is the shear stiffness given in Equation 1. For the calculation of shear stiffness, it is essential to correctly determine the moment of inertia of the cross-section (I) and the elasticity modulus (E) of the material. Although there are slight differences in actual, the modulus of elasticity is generally

Erdem DAMCI, Çağla ŞEKERCİ

Determination of the Dynamic Properties of SDOF and MDOF Shear Frames with Image Processing Technique...

accepted as an average value determined by the materials.

When calculating the column length, the clear distance between the midpoints of the floor alignments is taken as the length of the SDOF system. Another point to be noted is the holes opened at the mounting points for the floor to be added. The inertia of the holes was calculated and subtracted from the total moment of inertia since it would cause a decrease in shear stiffness (Equation 1). The period T and natural frequency f_n of the SDOF system is calculated by Equations 2 and 3, respectively.

$$k = 2 \times \frac{12EI}{L^3} \tag{1}$$

$$T_n = 2\pi\sqrt{\frac{m}{k}} \tag{2}$$

$$f_n = \frac{1}{T} \tag{3}$$

The frequency of the shaking table in harmonic loadings was determined by considering theoretical calculations, and in earthquake simulation, the Newmark Method [24] is used. The time histories are compared with relative root-mean-square error (relative RMS error) using Equation 4. Values below 10% are accepted as excellent accuracy.

$$\varepsilon_{rel} = \frac{\sqrt{(1/N)\sum_{n=1}^{N}\left(x_a[n] - x_d[n]\right)^2}}{\sqrt{(1/N)\sum_{n=1}^{N}\left(x_d[n]\right)^2}} \times 100 \tag{4}$$

x_a and x_d denote the achieved and measured displacement values, respectively, in Equation 4. N is the number of data points used to calculate the error.

3. RESULTS AND DISCUSSION

This study performed free vibration and shake table experiments for the given SDOF and two-story MDOF shear frames, and their comparison with numerical analysis is presented. Free vibration tests determined natural frequencies, and models were updated according to the experimental dynamic characteristics.

3.1. SDOF Shear Frame

The total mass of the SDOF shear frame is 1.590 kg, whereas the additional masses of the accelerometer and indicator LED are 70 g and 7.5 g, respectively. In the analytical calculation for determining the natural frequencies, considering the moving top floor, half weight of the shear frame and additional masses on the top floor are taken as lumped mass by 872.5 g.

The elasticity modulus of aluminium is taken as 70 GPa, and the net moment of inertia, excluding the screw holes, is 121.33 mm⁴. With these values, the system's bending stiffness (EI) and shear stiffness (k) are calculated as 8.493100 Nm² and 0.279997 kN/m, respectively. By using Equations 1-3, natural frequency of the shear frame is determined as 2.851 Hz depending on the lumped mass consideration at the top floor and the shear stiffness of the two columns (Table 1).

Table 1 Mechanical specifications of SDOF experimental model

Story height L [mm]	Total mass m [kg]	Shear stiffness k [kN/m]	Natural frequency f_n [Hz]
714	0.8725	0.279997	2.851

3.1.1. Free vibration tests

Synchronous video recording and acceleration measurements are given in Figure 7 and Figure 8. Dominant frequencies are obtained as 3.080 Hz and 3.088 Hz from the power spectrum, respectively. The closeness of the results indicates that the experimental frequencies obtained from the free vibration tests are reliable.

Erdem DAMCI, Çağla ŞEKERCİ

Determination of the Dynamic Properties of SDOF and MDOF Shear Frames with Image Processing Technique...
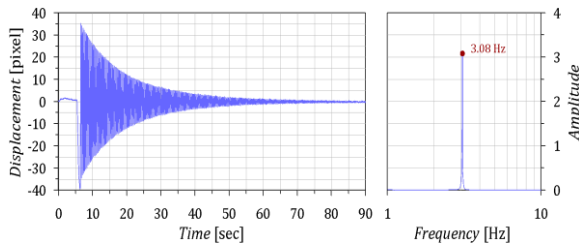
Figure 7 Displacement-time graph of the SDOF shear frame obtained by video processing (left) and calculated dominant frequency (right)
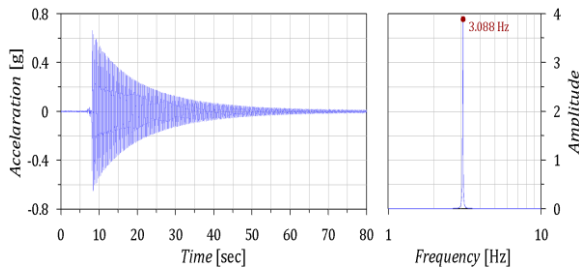
Figure 8 Acceleration-time graph of the SDOF shear frame obtained by vibration analysis (left) and calculated dominant frequency (right)

It was found that the difference between the frequencies was around 7.5%, leading to an error of about 14% in bending stiffness, comparing the experimental and analytical results (Table 2). Model updating is necessary for reliable numerical analysis according to the differences found in more than 5%. The comparison is given in Table 2 in detail. Damping ratios were determined from experimental results by the logarithmic decrement method for several cycles, and it was accepted as 0.40% on average.

3.1.2. Harmonic loading

Forced vibration tests were performed to determine the dominant frequency of the SDOF system, also considering nonlinear behaviour. Two different harmonic excitations were chosen for loading. The first test using the natural frequency of the shear frame (3.08 Hz, $\beta=1$) was carried out with an amplitude of ±0.5 mm to prevent damage due to amplification in the resonance state (Figure 9).

Table 2 Comparison of analytical and experimental results

	Analytical	Image Processing	Difference [%]	Vibration Analysis	Difference [%]
Frequency [Hz]	2.851	3.080	7.44	3.088	7.68
Damping Ratio [%]	-	0.396	-	0.406	-
EI [Nm^2]	8.4931	9.9115	14.31	9.9631	14.75

The second test was carried out using an amplitude of ±5 mm at 5 Hz, which is 1.6 times the resonance frequency. In both excitations, the harmonic response of the shear frame was measured by LEDs placed at the top floor level. Figures 9 and 10 show the displacement-time series with Power Spectrums. The shear frame exhibited similar responses for 3.08 Hz and 5 Hz excitation frequencies.
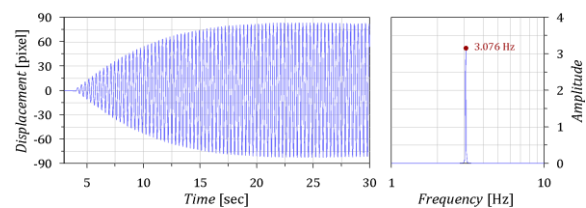
Figure 9 Displacement-time graph (left) and power spectrum (right) at top floor level (±0.5 mm @ 3.08 Hz, $\beta\approx1$)
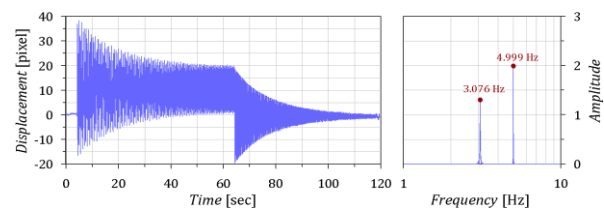
Figure 10 Displacement-time graph (left) and power spectrum (right) at top floor level (±5 mm @ 5 Hz, $\beta\approx1.6$)

Erdem DAMCI, Çağla ŞEKERCİ

Determination of the Dynamic Properties of SDOF and MDOF Shear Frames with Image Processing Technique...

3.1.3. Earthquake simulation

In earthquake simulations, the ground motion is scaled in order to comply with the shake table's displacement limits. Where the stroke limit of the table is ±75 mm, displacements of the 10/18/1989 Loma Prieta earthquake [25] were scaled to 1/15. The table performance under the relevant earthquake motion was evaluated by comparing the built-in linear potentiometer signal in the simulator and the data obtained via image processing.

Figure 11 presents the displacement-time graphs obtained by the image processing, the built-in linear potentiometer of the shake table, and the scaled ground (desired) motion. The comparisons between the time histories carried out by relative RMS errors (rRMSe) using Equation 4 are given in Table 3.
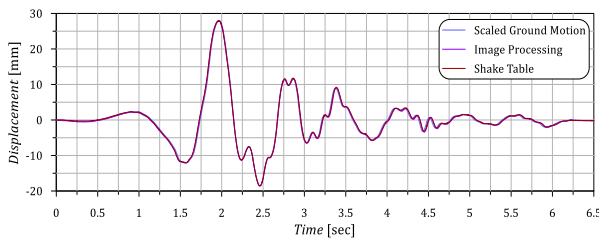
Figure 11 Comparison of recorded time histories with 10/18/1989 Loma Prieta earthquake simulation (Scale: 1/15)

Table 3 Comparison of table performance for experimental results

Time series		Time series	rRMSe [%]
Scaled Ground Motion	↔	Shake table	6.73
Scaled Ground Motion	↔	Image Processing	6.14
Shake table	↔	Image Processing	2.31

Both the performance of the shaking table and the displacement of the top floor level are compatible with the theoretical calculations for earthquake loading. Time-domain analyses under the 1/15 scale of the 1989 Loma Prieta earthquake was performed using the Newmark average acceleration method

and compared with the video recording analysis. The results of the experimental and numerical analysis are shown in Figure 12.

The relative RMS errors that are calculated between the scaled ground motion-shake table, Scaled ground motion-image processing, and Shake table-image processing are 6.73%, 6.14%, and 2.31%, respectively. These differences below 10% are considered negligible and indicate an excellent accuracy between the time series. Some reasons for differences between experimental and numerical results are discussed;

i. Manufacturing defects affecting the model behaviour and the differences between material properties taken into consideration in numerical analysis,

ii. Time lag occurred in earthquake simulations due to electronic components of the shake table [21],

iii.

iv. Errors due to centroid calculations of LED tracking.
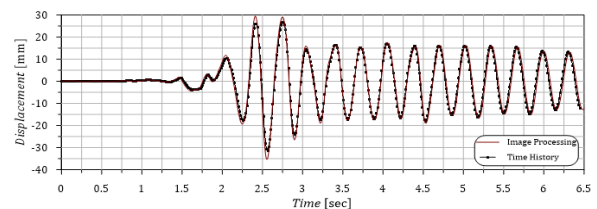
Figure 12 Comparison of image processing and time-history analysis obtained at the top floor under 1/15 scale 10/18/1989 Loma Prieta earthquake simulation

3.2. MDOF Shear Frame

Successful results were obtained with the image processing technique in the single-degree-of-freedom system. In order to examine the performance of the presented method in a multi-degrees-of-freedom system, the existing SDOF model was converted to a 2-degree-of-freedom shear frame by adding an intermediate floor. Similar to the SDOF system, the lumped masses on the floors and the shear stiffness of the frame were used in comparisons.

Erdem DAMCI, Çağla ŞEKERCİ

Determination of the Dynamic Properties of SDOF and MDOF Shear Frames with Image Processing Technique...

Taking into consideration the columns, additional masses (accelerometers, LED indicators) and rigid floor, the lumped masses of the floors and shear stiffness of the stories are given in Table 4. Considering these values, using MATLAB [23], Eigenvalue-eigenvector analyses were performed to determine the theoretical natural frequencies and mode shapes of the MDOF system. As a result of the analysis, the first mode frequency was determined as 5.88 Hz, and the second mode frequency was 14.68 Hz.

Table 4 Mechanical specifications of the MDOF experimental model

Story (i) Mode (n)	Height L_i [mm]	Mass m_i [kg]	Shear stiffness k_i [N/mm]	Modal frequency f_n [Hz]
1	357	0.873	2.61	5.88
2	357	0.674	2.61	14.68

3.2.1. Free vibration tests

Similar to the SDOF system, a free vibration test was carried out to determine the dominant frequency of the MDOF system. In Figure 13, the displacement-time graphs of the two floors of the structure were obtained by image processing and the dominant frequency was determined as 5.932Hz, representing the first mode. Due to low amplitudes of free vibration, the second mode frequency was not observed in the time domain. For the determination of the second mode, forced vibration tests were carried out, and the results are given in Section 3.2.2.

3.2.2. Harmonic loading

Harmonic excitations of ±2 mm @ 5.884 Hz and ±1 mm @ 16.455 Hz were applied to the MDOF shear frame on the shake table, determining the first and second mode frequencies. Figures 14 and 15 give the displacement-time histories of both tests obtained by image processing. The mode shapes and the resonance frequencies given in Figures 16-19 are determined by

experimental modal analyses using the transfer function. Figure 18 and Figure 19 show the comparison of the mode shapes. In Figures 18a and 19a, the instant photos taken from the video recordings, showing the maximum lateral displacements, represent the deformed shapes of the first and second modes, respectively. Mode shapes calculated by transfer function are given in Figures 18b and 19b, whereas the theoretical mode shapes obtained by eigenvalue-eigenvector analyses are given in Figures 18c and 19c. The same values are obtained between theoretical and experimental modal analysis results (difference= 0.34%) for the first mode frequency, where the experimental and theoretical mode shapes have a negligible difference of 0.92%. The second mode frequencies have a difference of 7.61%, where the difference between the mode shapes is 0.36%.

Differences of less than 1% may be attributed to one or more factors, such as image quality, measurement frequency, and manufacturing defects. Significantly, the difference in the second mode frequencies can be eliminated using the model update technique with the shear stiffnesses that can be defined separately for each story when the experimental results are taken as a basis.
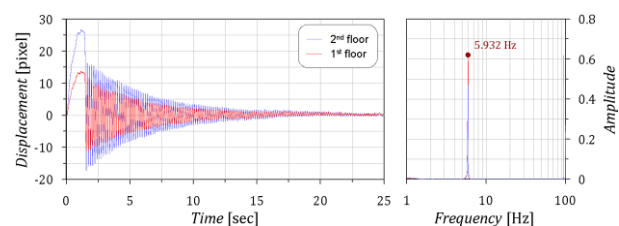
Figure 13 The displacement-time graph and power spectrum obtained by image processing
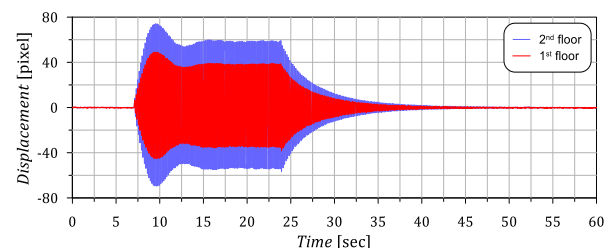
Figure 14 Displacement-time histories at floor levels (±2 mm @ 5.884 Hz β≈1)

Erdem DAMCI, Çağla ŞEKERCİ

Determination of the Dynamic Properties of SDOF and MDOF Shear Frames with Image Processing Technique...
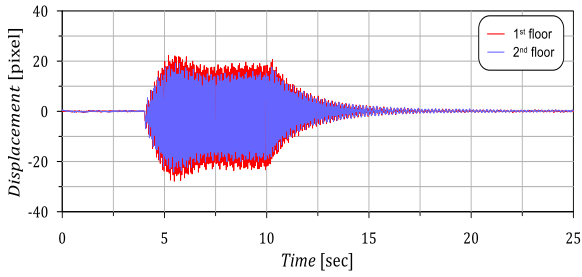
Figure 15 Displacement-time histories at floor
levels (±1 mm @ 16.455 Hz β≈1.12)
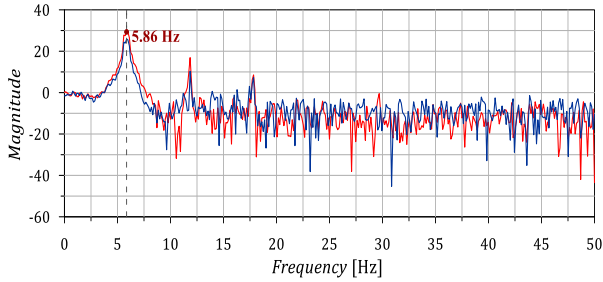
Figure 16 Determination of the dominant
frequency using transfer function
(±2 mm @ 5.884 Hz β≈1)
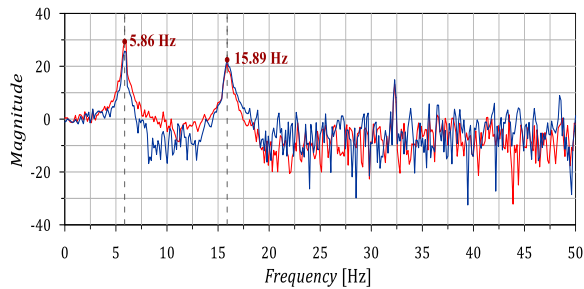
Figure 17 Determination of the dominant
frequencies using transfer function
(±1 mm @ 16.455 Hz β≈1.12)
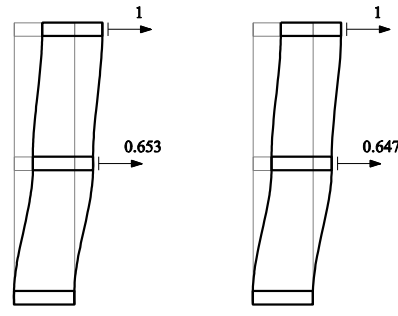
(a)   (b)   (c)

Figure 18 First mode shapes. a) Video frame
with maximum displacements, b) first mode
shape obtained experimentally, c) first mode
shape obtained theoretically.
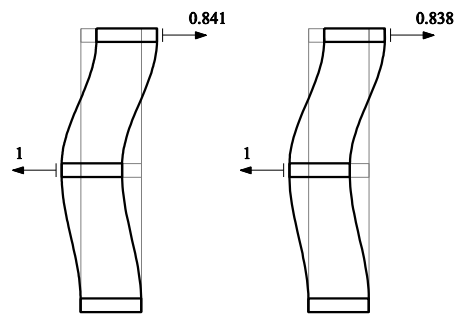
(a)   (b)   (c)

Figure 19 Second mode shapes. a) Video frame
with maximum displacements, b) second mode
shape obtained experimentally, c) second mode
shape obtained theoretically.

Erdem DAMCI, Çağla ŞEKERCİ

Determination of the Dynamic Properties of SDOF and MDOF Shear Frames with Image Processing Technique...

4. CONCLUSIONS

Due to its versatility, image processing has become a preferred technique for laboratory experiments. Especially in tests conducted in laboratory environments, LED tracking is an easy-to-implement tool besides instrumentation with other devices for measurement. White LEDs with high light intensity are ideal for image tracking and give satisfactory results. The technique proposed for determining each video frame's optimum median filter size gives reasonable results.

Using this technique for educational and research purposes without any instrumentation, dynamic behaviour and characteristics can be evaluated within the error range of 10% compared to high-cost laboratory equipment such as piezo sensors and DAQ devices. This paper shows that, for fundamental vibration analyses in structural dynamics, the presented technique can be easily used for determining the mode shapes and dominant frequencies of MDOF structural systems.

Authors' Contribution
The authors contributed equally to the study.

The Declaration of Conflict of Interest/ Common Interest
No conflict of interest or common interest has been declared by the authors.

The Declaration of Ethics Committee Approval
This study does not require ethics committee permission or any special permission.

The Declaration of Research and Publication Ethics
The authors of the paper declare that they comply with the scientific, ethical and quotation rules of SAUJS in all processes of the paper and that they do not make any falsification on the data collected. In addition, they declare that Sakarya University Journal of Science and its editorial board have no responsibility for any ethical violations that may be encountered, and that this study has not been evaluated in any academic publication environment other than Sakarya University Journal of Science.

REFERENCES

[1] C. S. Fraser, B. Riedel, "Monitoring the thermal deformation of steel beams via vision metrology", ISPRS Journal of Photogrammetry & Remote Sensing, vol. 55, pp. 268–276, 2000.

[2] G. A. Stephen, J. M. W. Brownjohn, C. A. Taylor, "Measurements of static and dynamic displacement from visual monitoring of the Humber Bridge", Engineering Structures, vol. 15, no. 3, pp. 197–208, 1993.

[3] K. Park, S. Kim, H. Park, K. Lee, "The determination of bridge displacement using measured acceleration", Engineering Structures, vol. 27, pp. 371–378, 2005.

[4] J. J. Lee, M. Shinozuka, "A vision-based system for remote sensing of bridge displacement", NDT&E International, vol. 39, pp. 425–431, 2006.

[5] R. Jiang, D. V. Jauregui, K. R. White, "Close-range photogrammetry applications in bridge measurement : Literature

Erdem DAMCI, Çağla ŞEKERCİ

Determination of the Dynamic Properties of SDOF and MDOF Shear Frames with Image Processing Technique...

review," Measurement, vol. 41, pp. 823–834, 2008.

[6] J. Park, J. Lee, H. Jung, H. Myung, "Vision-based displacement measurement method for high-rise building structures using partitioning approach", NDT and E International, vol. 43, no. 7, pp. 642–647, 2010.

[7] S. Kim, N. Kim, "Multi-point Displacement response measurement of civil infrastructures using digital image Processing", Procedia Engineering, vol. 14, pp. 195–203, 2011.

[8] Y. Yang, C. Dorn, T. Mancini, Z. Talken, G. Kenyon, C. Farrar, D. Mascareñas, "Blind identification of full-field vibration modes from video measu-rements with phase-based video motion magnification", Mechanical Systems and Signal Processing, vol. 85, pp. 567–590, 2017.

[9] J. Javh, J. Slavic, M. Boltez, "High frequency modal identification on noisy high-speed camera data", Mechanical Systems and Signal Processing, vol. 98, pp. 344–351, 2018.

[10] B. Kwan, J. Woo, Y. Kim, T. Cho, H. Seon, "Vision-based system identification technique for building structures using a motion capture system", Journal of Sound and Vibration, vol. 356, pp. 72–85, 2015.

[11] X. W. Ye, T. Yi, C. Z. Dong, T. Liu, "Vision-based structural displacement measurement : System performance evaluation and influence factor analysis", Measurement, vol. 88, pp. 372–384, 2016.

[12] S. Wang, B. Guan, G. Wang, Q. Li, "Measurement of sinusoidal vibration from motion blurred images", Pattern Recognition Letters, vol. 28, pp. 1029–1040, 2007.

[13] H. Choi, J. Cheung, S. Kim, J. Ahn, "Structural dynamic displacement vision system using digital image processing", NDT & E International, vol. 44, no. 7, pp. 597–608, 2011.

[14] J. G. Chen, N. Wadhwa, Y. Cha, F. Durand, W. T. Freeman, "Modal identification of simple structures with high-speed video using motion magnifi-cation", Journal of Sound and Vibration, vol. 345, pp. 58–71, 2015.

[15] J. G. Chen, N. Wadhwa, F. Durand, W. T. Freeman, O. Buyukozturk, "Develop-ments with Motion Magnification for Structural Modal Identification Through Camera Video", Dynamics of Civil Structures, Conference Proceedings of the Society for Experimental Mechanics Series, vol. 2, pp. 49–57, 2015.

[16] P. L. Reu, D. P. Rohe, L. D. Jacobs, "Comparison of DIC and LDV for practical vibration and modal measu-rements", Mechanical Systems and Signal Processing, vol. 86, pp. 2–16, 2017.

[17] C. Rinaldi, J. Ciambella, V. Gattulli, "Image-based operational modal analysis and damage detection validated in an instrumented small-scale steel frame structure", Mechanical Systems and Signal Processing, vol. 168, no. May 2021, p. 108640, 2022.

[18] D. Feng, M. Q. Feng, "Experimental validation of cost-effective vision-based structural health monitoring", Mechanical Systems and Signal Processing, vol. 88, no. November 2016, pp. 199–211, 2017.

[19] H. Chung, J. Liang, S. Kushiyama, M. Shinozuka, "Digital image processing for nonlinear system identification", International Journal of Non-Linear Mechanics, vol. 39, pp. 691–707, 2004.

Erdem DAMCI, Çağla ŞEKERCİ

Determination of the Dynamic Properties of SDOF and MDOF Shear Frames with Image Processing Technique...

[20] C. T. Do Cabo, N. A. Valente, Z. Mao, "A Comparative Analysis of Imaging Processing Techniques for Non-Invasive Structural Health Monitoring", IFAC-PapersOnLine, vol. 55, no. 27, pp. 150–154, 2022.

[21] E. Damcı, Ç. Şekerci, "Development of a Low-Cost Single-Axis Shake Table Based on Arduino", Experimental Techniques, vol. 43, no. 2, pp. 179–198, 2019.

[22] S. Antoniou, R. Pinho, F. Bianchi, "SeismoSignal" 2008.

[23] Matlab, "version 2017b" The MathWorks, Inc., Natick, 2017.

[24] A. K. Chopra, Dynamics of Structures Theory and Applications to Earthquake Engineering, Englewood Cliffs, New Jersey: Prentice-Hall, Inc., 1995.

[25] PEER Center. (2016, Feb. 01). PEER Ground Motion Database [Online]. Available: http://ngawest2.berkeley.edu/